

## AMB Express

### Towards the Understanding of the Enzymatic Cleavage of Polyisoprene by the Dihaem-Dioxygenase RoxA

#### Additional file 1

*Georg Schmitt, Jakob Birke\* and Dieter Jendrossek*

*Institute of Microbiology, University of Stuttgart, Germany*

*\*present address: Institute of Applied Biotechnology, University of Applied Sciences  
Biberach, Hubertus-Liebrecht-Strasse 35, 88400 Biberach, Germany*

\*Correspondent footnote: Dieter Jendrossek

Institut für Mikrobiologie

Universität Stuttgart

Allmandring 31

70569 Stuttgart

Germany

Tel.: +49-711-685-65483

Fax: +49-711-685-65725

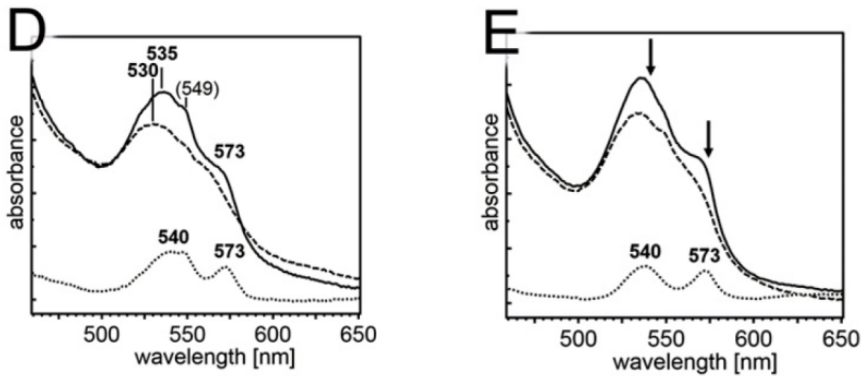
E-mail: [dieter.jendrossek@imb.uni-stuttgart.de](mailto:dieter.jendrossek@imb.uni-stuttgart.de)

or [imbdj@imb.uni-stuttgart.de](mailto:imbdj@imb.uni-stuttgart.de)

**Additional file 1: Table S1: Effect of potential external haem ligands like imidazole and related low molecular compounds on activity and on UVvis-properties of RoxA-Wt as *isolated*** (originally published in Schmitt et al. 2010).

Compound	Structure	Maximum (Soret-band) [nm]	Maximum (Soret-band) in difference spectrum [nm]	Intensity of Soret band in difference spectrum [mAU]	Velocity of effect	Residual activity [%]			
						10mM	1mM	100µM	10µM
Imidazole		407 + 417	418	140	fast	< 10	15	45	85
1-Methyl-imidazole		407 + 417	418	145	fast	< 10	< 10	40	nd
2-Methyl-imidazole		407	(418)	10	slow	75	> 95	> 95	nd
1,2-Dimethyl-imidazole		407	(418)	10	very slow	50	90	> 95	nd
Pyrazole		412	416	90	very fast	< 10	45	90	nd
(3,5)- Dimethylpyrazole		407	415-416	25	slow			95	90
Pyrrole		407	-	< 5	no effect		> 95	> 95	nd
Pyrazine		411	415	70	very fast	10	10	30	nd
2-Methyl-pyrazine		411	415	90	very fast		10	40	nd
2,5-Dimethyl-pyrazine		407	414	10	no effect		90	95	nd
Pyridine		413-414 (with shoulder at 407)	416	100	very fast	< 5	5	10	nd
2-Methyl-pyridine		407	-	< 5	no effect		85	90	nd
4-Methyl-Pyrimidine		412	415	100	medium		10	35	nd
Pyridazine		410	415	60	fast		45	90	nd
Pyrrolidine		411	418	85	slow		80	90	nd
Methimazole		407	-	< 5	no effect	95	> 95	> 95	nd
Hydrazine	H <sub>2</sub> N – NH <sub>2</sub>	407 (general decrease of absorption)	416	10	slow	< 5	< 5	< 5	5

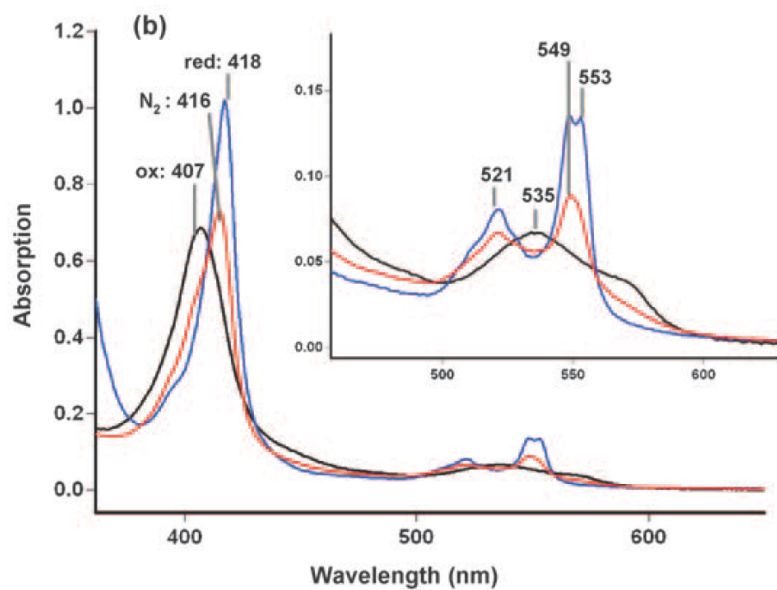
Results of UVvis spectroscopy and activity assays of RoxA in the presence of imidazole and structurally related, N-containing compounds under oxic conditions are given. RoxA as isolated has a Soret maximum at 407 nm. All optical investigations were performed at a RoxA concentration of 2  $\mu$ M. The Soret maxima in the absolute UVvis spectrum and the spectral changes in difference spectrum [RoxA in the presence of the test compound minus RoxA as isolated] are listed, as well as the order of velocity of the effects. The intensity of the change of Soret band in difference spectrum can be compared to a total intensity of about 350 mAU with fully reduced RoxA (Na-dithionite) at 418 nm. Activity assays were performed as described in the methods section in 100 mM potassium phosphate buffer (pH 7.0) with incubation for 3 hours. The residual activities are shown in % of the untreated control (RoxA without compounds). Not determined (nd), no significant change (-).



**Additional file 1: Fig. S1: RoxA incubated with ferricyanide (left) or pyrogallol (right)** (originally published in Fig. 4D, E of (Seidel et al. 2013))

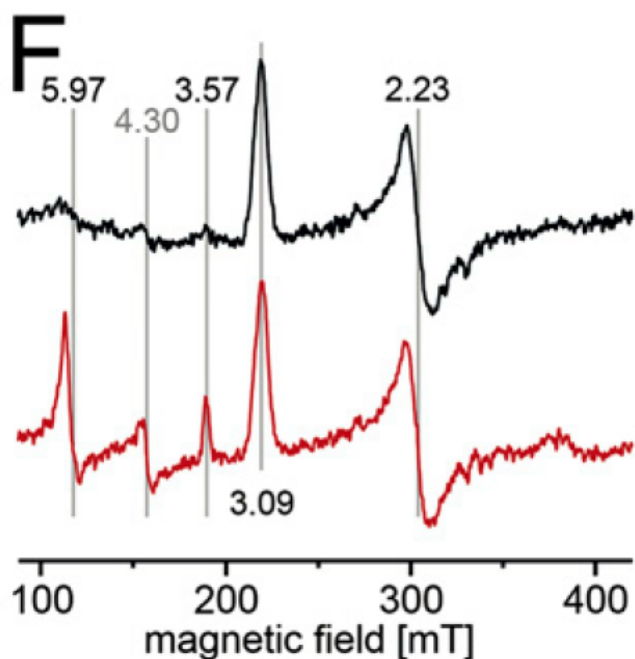
After incubation of RoxA as *isolated* (solid line) with ferricyanide, distinct UVvis features that are typical for a  $\text{Fe}^{3+}$  spectrum are observed (dashed line). The difference spectrum (dotted line) visualises signals at 540 and 573 nm.

A similar effect is observed when RoxA as *isolated* (solid line) is treated with pyrogallol to remove bound  $\text{O}_2$  (dashed line). Arrows indicate a loss of absorption on removal of dioxygen.



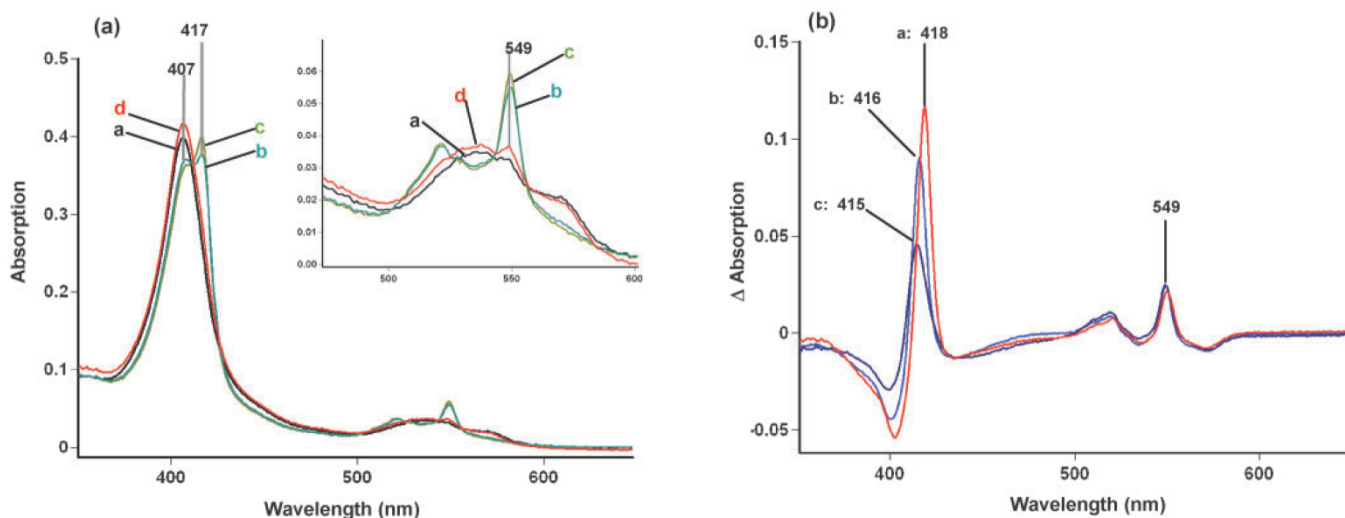
**Additional file 1: Fig. S2: UVvis spectra of RoxA.**

RoxA as isolated (black), dithionite-reduced (blue) and incubated under N<sub>2</sub> atmosphere (red) for 48h (originally published in Fig. 1b of (Schmitt et al. 2010)). The increasing 549 nm  $\alpha$ -band visualises a pseudo-reduction of the N-terminal haem centre under low oxygen gas pressure because of the reversible removal of dioxygen. In this case, a ferrous iron is left that can be reoxygenated under air atmosphere.



**Additional file 1: Fig. S3: EPR spectra of RoxA.**

RoxA *as isolated* (black) and reoxidised RoxA (red, dithionite reduced and subsequently reoxidised with ferricyanide) (originally published in Fig. 4F of {Seidel:2013eu}). The C-terminal haem group rests in the oxidised state, therefore it can be seen in the *as isolated* spectrum ( $g = 3.09, 2.23, \sim 1.5$ ). The reduced, dioxygen bound N-terminal haem centre is EPR silent (black). After reoxidation, this haem is visible as two different species, one *high spin* state that probably corresponds to a 5-fold ligated state ( $g = 5.97$ ) and a new low spin species ( $g = 3.57$ ) that is most likely 6-fold coordinated (red). The sixth coordination sphere might be occupied by an unknown distal ligand. The signal at  $g = 4.3$  refers to non-specifically bound iron(III).



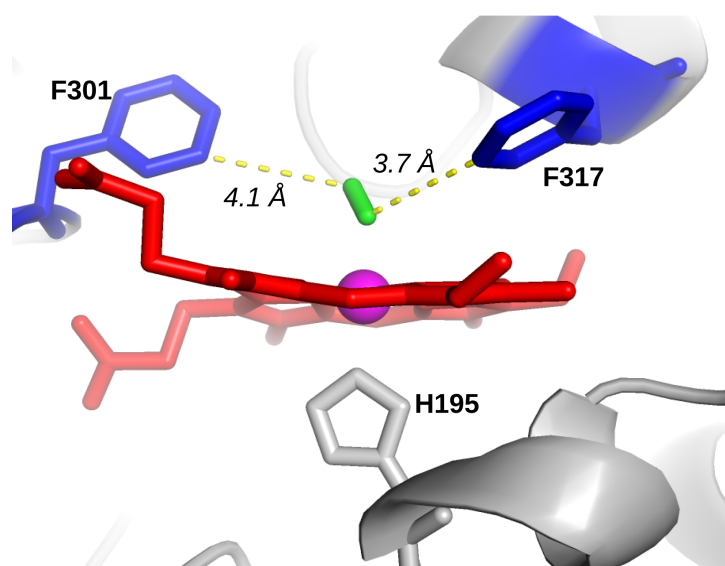
**Additional file 1: Fig. S4: RoxA incubated with different haem ligands**

(originally published in Fig. 3 of (Schmitt et al. 2010)).

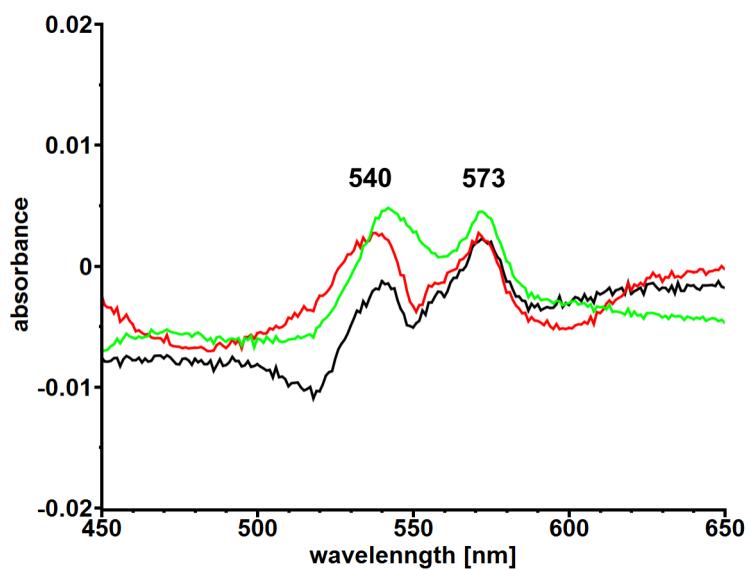
(a) UV/vis spectra of RoxA as *isolated* (a, black line) and RoxA in the presence of 1 mM imidazole (b, blue), 1-methylimidazole (c, green) and 2-methylimidazole (d, red), incubated for 1 h at room temperature under air. A double Soret maximum at 407 and 417 nm and an  $\alpha$ -band at 549 nm (inset) appeared after the addition of imidazole and 1-methylimidazole.

(b) Difference spectra (RoxA-ligand minus RoxA as *isolated*) with imidazole (a, red), pyridine (b, black) and pyrazine (c, blue) at the end point of the reaction (all under air atmosphere).

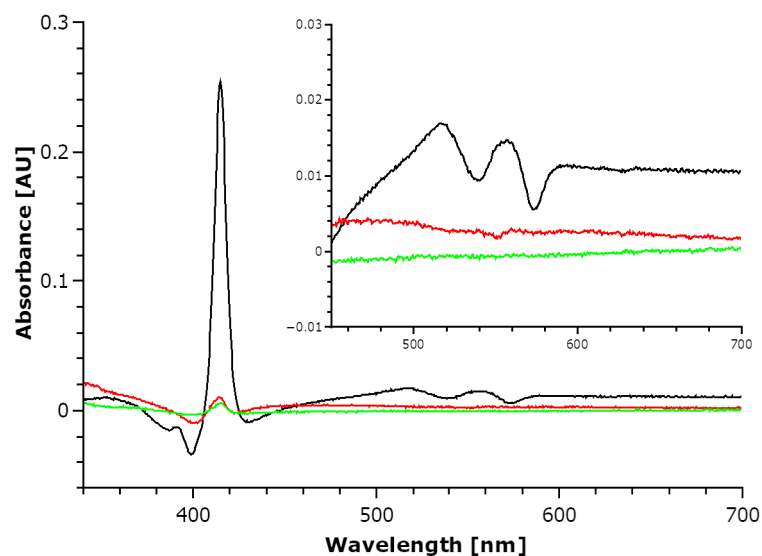
The effects of most ligands (with exception of 2-methylimidazole) can be explained by ligand binding to the N-terminal haem centre, thereby substituting dioxygen as axial distal ligand. As a result, the spectra show characteristics of an oxidised (C-terminal,  $\text{Fe}^{3+}$ ) as well as a reduced state (N-terminal:  $\text{Fe}^{2+}$ -ligand). 2-methylimidazole cannot substitute  $\text{O}_2$ , possibly the methyl group leads to a steric hindrance that prevents a binding to the haem.



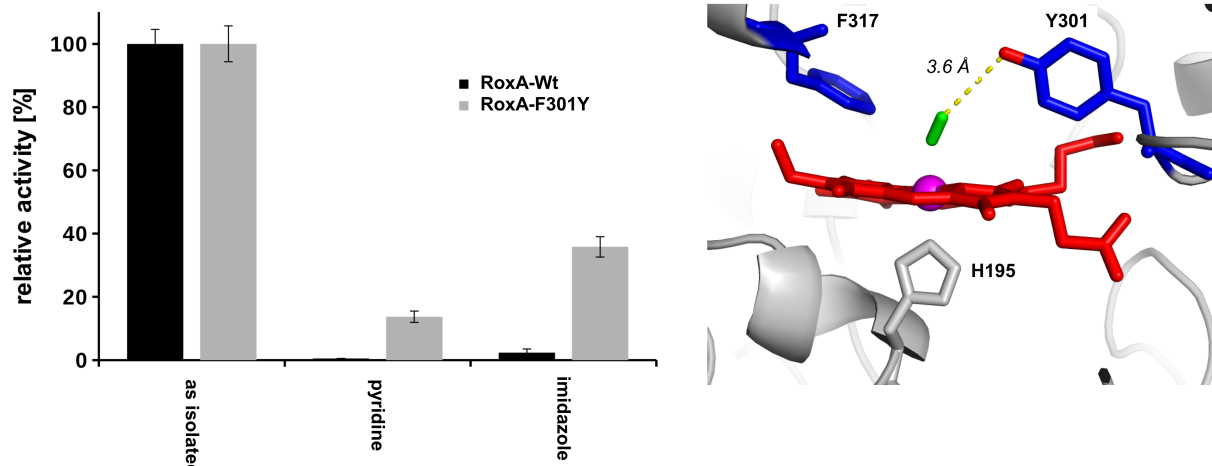
**Additional file 1: Fig. S5: Part of the RoxA active site.** The distal haem pocket of the catalytic N-terminal haem centre (red) consists of hydrophobic amino acid side chains. The residues F301 and F317 (blue) are in close vicinity to the haem-bound dioxxygen molecule (green). The two axial ligands are shown in grey (H195) and green (dioxxygen).



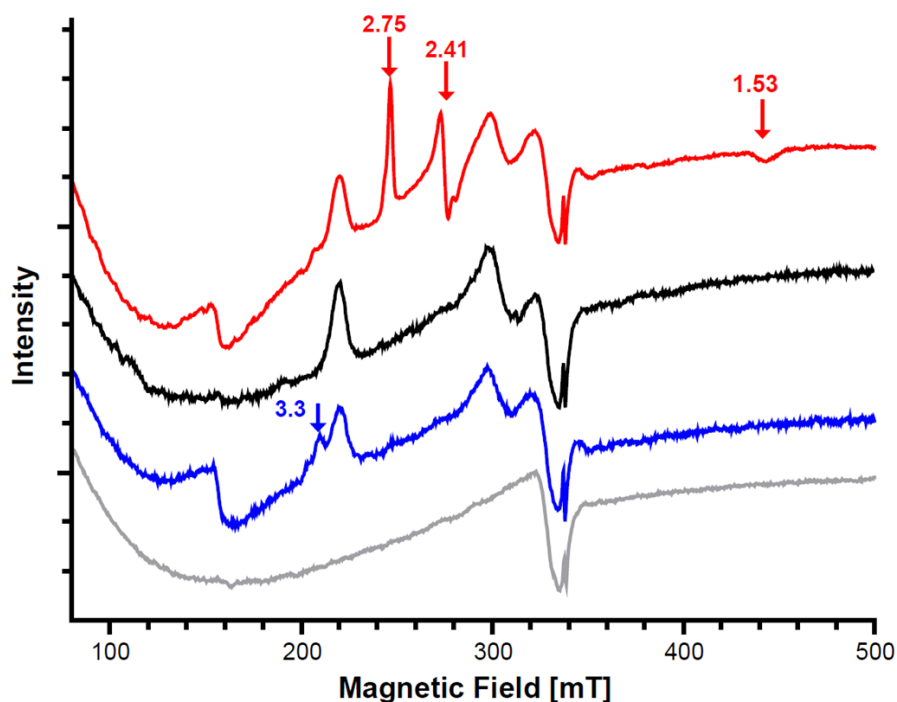
**Additional file 1: Fig. S6: Comparison of UVvis spectra of RoxA Wt and RoxA-F317A.** UVvis difference spectra of RoxA-Wt minus RoxA-F317L (black), RoxA-F317Y (red), RoxA-F317A (green) in the Q-band regions. The difference spectra show decreased absorptions of the muteins at 540 nm and 573 nm. These are characteristic for oxidised N-terminal haem centres, thus without bound dioxygen as in RoxA-Wt as isolated (compare **Fig. 1**).



**Additional file 1: Fig. S7: Reaction of RoxA-Wt and RoxA-F317Y with carbon monoxide.** UVvis difference spectrum of RoxA-Wt incubated with CO-buffer minus RoxA-Wt as isolated (compare Fig. 6 of (Birke et al. 2015)), oxidised RoxA-Wt + CO minus oxidised RoxA-Wt (red) and RoxA-F317Y + CO minus RoxA-F317Y as isolated (green). The Q-Bands are enlarged (inset). The spectral changes indicate a release of haem-bound dioxygen and a binding of CO to the ferrous N-terminal haem centre of RoxA-Wt. Only minor changes appeared with both oxidised RoxA-Wt and RoxA-F317Y, which indicates the ferric nature of the respective haem centre.



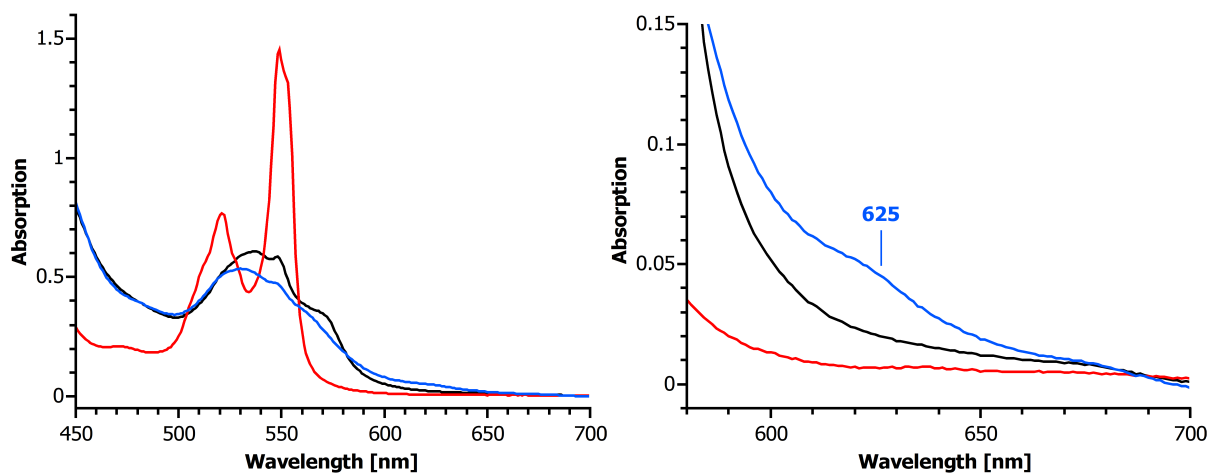
**Additional file 1: Fig. S8: (left) Effect of pyridine and imidazole on the activity of RoxA-F301Y.** Relative activities of RoxA-Wt and RoxA-F301Y (both set to 100%) in the presence of pyridine or imidazole (2 mM). The activity of RoxA-F301Y was 21% of RoxA-Wt. The haem ligands have a weaker effect on the activity of RoxA-F301Y compared to RoxA-Wt. **(right)** The haem pocket of the N-terminal haem centre of RoxA-F301Y (different view compared to **suppl. Fig. S6**). The structure was modelled with the SWISS model server (Biasini et al. 2014) based on the RoxA-Wt structure (pdb: 4B2N). Tyrosine 301 stabilises the haem-bound dioxygen molecule (green) with a hydrogen bond, leading to decreased activity.



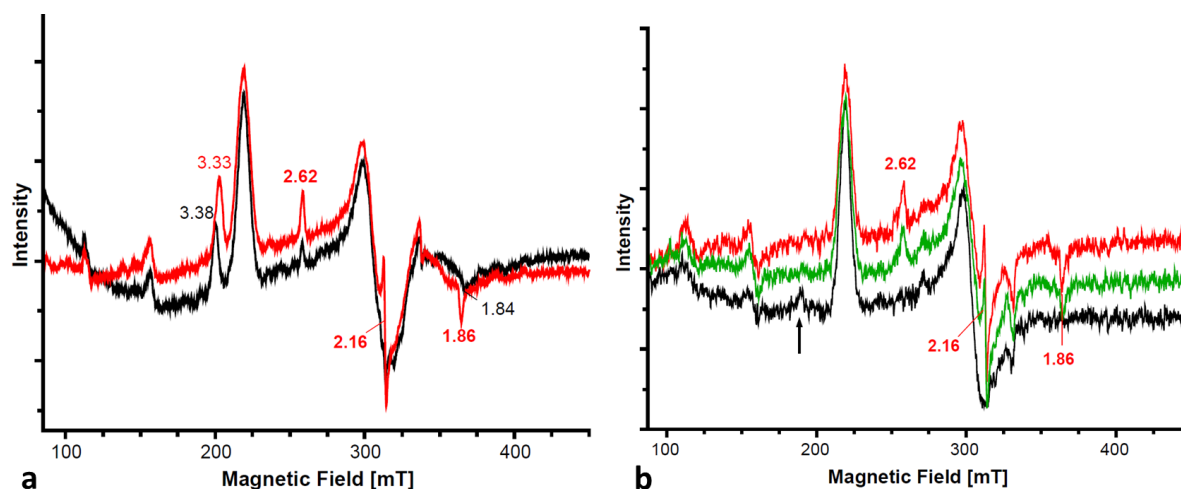
**Additional file 1: Fig. S9: EPR spectra of RoxA.** The spectra were recorded at 10 K of RoxA as *isolated* (black), RoxA in NO-saturated buffer (red, 5 min) and this sample after addition of pyridine (5 mM, 15 min) (blue). Reaction of RoxA as *isolated* with NO resulted in a new rhombic species at  $g_z=2.75$ ,  $g_y=2.41$ , and  $g_x=1.53$ . This species completely disappeared by addition of pyridine while the characteristic pyridine-ligated low-spin signal at  $g=3.3$  formed at the same time. These spectra are shown without cavity-subtraction for a better resolution of the haem signals. For comparison, a spectrum of buffer only is shown (gray).

Besides in porphyrin models in organic solvents such a rhombic low temperature species at  $g_z=2.75$ ,  $g_y=2.45$ , and  $g_x=1.53$  has not been described for a NO-derived enzyme-bound haem species, so far, to our knowledge. This species is much distinct to a ferrous-NO ligation, the anisotropy is similar to a nitrite-coordination and rather reminds of a peroxy-nitrite ferrihaem complex (Sharma et al. 2017). Interestingly, bis-(nitro-)/*low-spin* species as described with porphyrin model systems (Munro and Scheidt, 1998; Nasri et al., 1990; Lyakin et al. 2009) fit very well the observed species, but comparability to RoxA is limited. The binding of nitric oxide often leads to lability or even rupture of the *proximal* (His-) N-Fe bond (e. g. e.g. Reynolds et al. 2000; Rodgers et al. 2000;), the generation of a bis-NO<sub>2</sub><sup>-</sup>-coordination at the N-terminal haem of RoxA is unlikely.

We provided evidence that a ferric N-terminal haem is formed in a first reaction from RoxA-WT (O<sub>2</sub>-ligated) with NO. Since *high-spin* signals were completely absent in the respective EPR- and UVvis spectra, we propose a further reaction of this ferric haem with additional NO or NO<sub>2</sub><sup>-</sup>/NO<sub>3</sub><sup>-</sup>, which could be formed by reaction of ferric haem with NO resulting in nitrite (NO + H<sub>2</sub>O/OH<sup>-</sup> → NO<sub>2</sub><sup>-</sup>). Also, a reaction of the proposed intermediate peroxy-nitrite (eq. (1)) with Phe317 close to the distal coordination site in RoxA WT or Tyr in RoxA-F317Y must be taken into account: nitrophenylalanine or *p*-nitrotyrosine, respectively, could be formed (Beckmann and Koppenol, 1996; Alvarez and Radi, 2003) and serve as the haem distal ligand. Because the UVvis signals could be interpreted as ferric-NO derived, but not the EPR spectra, a distinct conformation appearing upon freezing to low temperature (10 K) may be considered.



**Additional file 1: Fig. S10: Optical spectrum of RoxA after reduction and reoxidation under anaerobic conditions (enlarged on the right).** When RoxA as *isolated* (black) is reduced (red) and subsequently ferricyanide-reoxidised (blue), an additional weak absorption increase upon ferricyanide-reoxidation around 625 nm can be observed, indicating a *high-spin* coordination at the N-terminal haem centre directly after reoxidation.



**Additional file 1: Fig. S11: EPR spectra of RoxA-Wt in the presence of small substrate analogues. (a)** RoxA-Wt as isolated from rubber latex culture (black) and after addition of  $\beta$ -carotene (2 mM, red). A rhombic *low-spin* species with  $g$ -values of 2.62, 2.16 and 1.86, indicating a haem-O-X coordination, was increasing in presence of  $\beta$ -carotene and another *low-spin* species at  $g=3.38$  (strong ligand), attributed to the same (N-terminal) haem, was shifted. **(b)** From recombinant RoxA-Wt (black) the same species at  $g=2.62$ , 2.16 and 1.86 appeared by addition of pristane (2 mM, red) or squalene (2 mM, green), respectively, and a minor *low-spin* signal (black arrow) disappeared.

## References

- Alvarez B and Radi R. (2003) Peroxynitrite reactivity with amino acids and proteins. *Amino Acids* 25:295–311. doi: 10.1007/s00726-003-0018-8
- Biasini, M., Bienert, S., Waterhouse, A., Arnold, K., Studer, G., Schmidt, T., et al. (2014). SWISS-MODEL: modelling protein tertiary and quaternary structure using evolutionary information. *Nucleic Acids Research*, 42(W1), W252–W258. <http://doi.org/10.1093/nar/gku340>
- Beckmann JS and Koppenol WH. (1996) Nitric oxide, superoxide, and peroxynitrite: the good, the bad, and the ugly. *Am J Physiol*. 271:C1424-C1437.
- Birke J, R other W, Jendrossek D (2015) Latex clearing protein (Lcp) of *Streptomyces* sp. strain K30 is a *b*-Type cytochrome and differs from rubber oxygenase A (RoxA) in its biophysical properties. *Appl Environ Microbiol* 81:3793–3799. doi: 10.1128/AEM.00275-15
- Lyakin, O.Y., Bryliakov, P.K., Britovsek, G.J.P. and Talsi, E.P. (2009) EPR Spectroscopic Trapping of the Active Species of Nonhaem Iron-Catalysed Oxidation. *J Am Chem Soc*. 131, 10798–10799.
- Munro OQ and Scheidt WR (1998) (Nitro)Iron(III) Porphyrins. EPR detection of a transient *low-spin* Iron(III) complex and structural characterization of an O atom transfer product. *Inorg. Chem*. 37:2308-2316.
- Nasri HN, Goodwin JA, Scheidt WR (1990). Use of protected binding sites for nitrite binding in Iron(II) porphyrinates. Crystal structure of the bis(nitro)(a,a,a,a-tetrakis(o-pivalamidophenyl)porphinato)iron(III) anion. *Inorganic Chemistry* 29(2):185-191.
- Reynolds M F, Parks R B, Burstyn J N, Shelver D, Thorsteinsson M V, Kerby R L, Roberts G P, Vogel K M and Spiro T G (2000). Electronic absorption, EPR, and Resonance Raman

spectroscopy of CooA, a CO-sensing transcription activator from *R. rubrum*, reveals a five-coordinate NO-haem. *Biochemistry* 39, 388-396

Rodgers KR, Lukat-Rodgers GS, Tang L (2000) Nitrosyl adducts of FixL as probe of haem environment. *J Biol Inorg Chem* 5:642-654. doi: 10.1007/s007750000150

Schmitt G, Seiffert G, Kroneck PMH, Braaz R, Jendrossek D (2010) Spectroscopic properties of rubber oxygenase RoxA from *Xanthomonas* sp., a new type of dihaem dioxygenase. *Microbiology* (Reading, Engl) 156:2537–2548. doi: 10.1099/mic.0.038992-0

Seidel J, Schmitt G, Hoffmann M, Jendrossek D, Einsle O (2013) Structure of the processive rubber oxygenase RoxA from *Xanthomonas* sp. *Proc Natl Acad Sci USA* 110:13833–13838. doi: 10.1073/pnas.1305560110

Sharma SK, Schaefer AW, Lim H, Matsumura H, Moëne-Loccoz P, Hedman B, Hodgson KO, Solomon EI, Karlin KD (2017) A six-coordinate peroxynitrite low-spin iron(III) porphyrinate complex- The product of the reaction of nitrogen monoxide ( $\cdot\text{NO}(\text{g})$ ) with a ferric-superoxide species. *J Am Chem Soc* 139:17421–17430. doi: 10.1021/jacs.7b08468